 Nucleic Acids Research, 1999, Vol. 27, No. 11 **2387–2392**

2′-Pyrene modified oligonucleotide provides a highly sensitive fluorescent probe of RNA

Kazushige Yamana, Reiko Iwase[1], Shigeyuki Furutani[1], Hiroto Tsuchida[1], Hirofumi Zako, Tetsuji Yamaoka[1] and Akira Murakami[1,*]

Department of Applied Chemistry, Himeji Institute of Technology, 2167 Shosha, Himeji, Hyogo 671-2201, Japan and [1]Department of Polymer Science and Engineering, Kyoto Institute of Technology, Matsugasaki, Sakyo-ku, Kyoto 606-8585, Japan

Received January 25, 1999; Revised and Accepted April 12, 1999

ABSTRACT

Oligonucleotide 9mers containing 2′-O-(1-pyrenylmethyl)uridine [U(pyr)] at the center position were synthesized by using a protected U(pyr) phosphoramidite. The UV melting behaviors indicate that the pyrene-modified oligonucleotides can bind to both their complementary DNA and RNA in aqueous solution. When compared with the unmodified oligonucleotides, the pyrene-modified oligonucleotides showed higher affinity for DNA while exhibiting lower affinity for RNA. The pyrene-modified oligonucleotides in diluted solution exhibited fluorescence typical of pyrene monomer emission [λ_{max} 378 (band I) and 391 nm (band III)]. When these oligomers bound to DNA, the fluorescence intensity ratio of band III/band I was increased. With this fluorescence change, a new broad emission (λ_{max} 450 nm) due to exciplex between the pyrene and an adjacent nucleobase appeared. In contrast, addition of RNA to the pyrene oligonucleotides resulted in enhancement of the pyrene monomer emission with decrease in the fluorescence band ratio. The extent of the emission enhancement was found to be highly dependent on the nucleobase adjacent to the U(pyr) in the pyrene oligomers. The pyrene oligonucleotide containing dC at the 3′-site of the modification showed remarkable increase (~250 times) in fluorescence (375 nm) upon binding to complementary RNA. The present findings would open the way to the design of a highly sensitive fluorescent probe of RNA.

INTRODUCTION

The design and synthesis of fluorescent labeled oligonucleotides which display an enhanced signal upon hybrid formation have been the subject of intense research, since this type of oligonucleotide derivative can be used for solution-based analysis of nucleic acid sequences and RNA secondary and ternary structures. One possible approach involves the use of fluorescence polarization which increases upon duplex formation of fluorescein-labeled oligonucleotides with DNA (1). Another approach has been demonstrated by the suitable pairs of labeled oligonucleotides that exhibit characteristic emission derived from fluorescence resonance energy transfer upon binding to complementary DNA (2–5). It has been shown that fluorescent DNA binding agents such as oxazole yellow (6), rhodium complex (7) and Hoechst dye (8) linked oligonucleotides exhibit enhanced emission on hybrid formation with specific nucleic acid sequences. The oligonucleotide attached to a hydrophobic fluorescent dye has been shown to be useful for detection of DNA sequences by use of an enhanced fluorescence signal upon hybridization (9).

Among several fluorophores, the pyrene has been one of the attractive fluorescent dyes for development of a sensitive probe of DNA and RNA. Recent reports (10–14) have shown the utility of pyrene excimer emission in which binding of excimer-forming probes to DNA resulted in a considerable increase in the excimer emission. However, applications of the monomer emission have generally been limited, since the pyrene attached to oligonucleotides displayed moderate and poor fluorescence especially upon binding to DNA segments (15–17). The enhanced pyrene monomer emission upon binding to RNA segments has been reported for oligoribonucleotides carrying a pyrenyl group at the 5′-terminus, which was dependent on the environment of the probe–oligomer complexes (18). The fluorescence intensity change has been shown to be useful for studies of binding and dynamics involving RNA (19).

We have been interested in the development of a pyrene-labeled oligonucleotide probe possessing the properties whereby its binding to an RNA sequence resulted in the detectable emission changes in homogeneous solution (20–23). The method for the synthesis of pyrene-labeled oligonucleotides involves the incorporation of a pyrene fluorophore via a short tether into the 2′-O-position of oligonucleotides (20). The important feature of our method is that the pyrene can be placed anywhere in the sequence. It has already been shown that the oligopyrimidines containing 2′-pyrenylmethyluridine at the 5′-end exhibit enhanced pyrene monomer emission upon hybrid formation with poly(rA) (21). To establish the generality of this finding, we have investigated the properties of the pyrene-modified oligonucleotides focusing on the sequence effect on the fluorescence (22–23). In this paper, we describe that the oligonucleotide modified with one pyrenyl residue at the appropriate sequence exhibits remarkably enhanced monomer emission upon binding to a RNA segment. The present findings would open the way to the design of a highly sensitive fluorescent probe of RNA.

*To whom correspondence should be addressed. Tel/Fax: +81 75 724 7814; Email: akiram@ipc.kit.ac.jp

MATERIALS AND METHODS

General methods

^{31}P NMR spectra were measured on a JEOL-JNM-GX-400 spectrometer using 85% H_3PO_4 as an external standard. High-performance liquid chromatography (HPLC) was performed on a Shimadzu LC 6A equipped with a UV detector at 260 nm, using a reversed phase Wakosil 5C-18 200N (4.6 × 150 mm). Column chromatography and thin-layer chromatography (TLC) were carried out on Wako silica gel C-300 and Merck 60 PF_{254}, respectively. Ultraviolet (UV) spectra were recorded with a Hitachi U-2000A spectrophotometer equipped with a Hitachi SPR-10 thermoelectrically controlled cell holder. Circular dichroism (CD) spectra were obtained on a JASCO CD J-720 spectrophotometer equipped with a Neslab RTE-100 thermocontroller. Fluorescence spectra were measured with a Shimadzu RF5300PC spectrophotometer equipped with a Neslab RTE-100 thermocontroller.

Materials and solvents

5′-O-Dimethoxytrityl-2′-O-(1-pyrenylmethyl)uridine [5′-DMT-U(pyr)] was synthesized in a manner previously described (20). 2-Cyanoethyl N, N, N′, N′-tetraisopropylphosphoramidite was obtained from Aldrich Chemical Co. Protected deoxy- and ribonucleoside 3′-O-(2-cyanoethyl)-N,N-diisopropylphosphoramidites and nucleoside-loaded CPG supports were purchased from ABI and Cruachem. DNA and RNA oligomers were prepared by a standard phosphoramidite chemistry on an ABI 391 DNA/RNA synthesizer. Nuclease P1 and alkaline phosphatase were purchased from Wako Chemical Co. and Takara. Acetonitrile, dichloromethane and diisopropylamine were dried by refluxing with CaH_2 for at least 5 h under a nitrogen atmosphere, then distilled and stored over molecular sieves or CaH_2.

Synthesis of 5′-O-dimethoxytrityl-2′-O-(1- pyrenylmethyl)-uridine-3′-O-(2-cyanoethyl)-N,N-diisopropylphosphoramidite (5′-DMT-U(pyr) amidite)

2-Cyanoethyl N, N, N′, N′-tetraisopropylphosphoramidite (0.7 ml, 2.2 mmol) was added to a solution of 5′-DMT-U(pyr) (600 mg, 0.79 mmol), tetrazole (39 mg, 0.55 mmol) and diisopropylamine (78 µl, 0.55 mmol) in dry dichloromethane (4 ml). The solution was stirred at room temperature for 2 h. After addition of MeOH (1 ml) followed by diisopropylethylamine (0.15 ml) and ethylacetate (3 ml), the resulting solution was washed with 10% $NaHCO_3$ (4 ml × 3). After the organic layer was dried with Na_2SO_4, the solution was directly applied to a silica gel column. Elution was carried out with dichloromethane-ethylacetate-triethylamine (45:45:10, v/v). The appropriate fractions were collected and solvent was removed under reduced pressure to give a pale yellow powder (621 mg, 80.4%). 5′-DMT-U(pyr) amidite: TLC (CH_2Cl_2-EtOAc-Et_3N 45:45:10, v/v) Rf 0.60; ^{31}P NMR (CH_3CN) 150.3, 149.8 p.p.m. (diastereoisomers).

Synthesis of pyrene-modified oligonucleotides

Pyrene-modified oligonucleotides were synthesized by phosphoramidite chemistry beginning with 5′-DMT-T (1 µmol) bound to a CPG support. For the coupling of normal deoxyribonucleoside phosphoramidites, the standard protocol (50 µl of 0.1 M amidite and 50 µl of 0.1 M tetrazole in acetonitrile, 2 min) was used on a DNA synthesizer. For 5′-DMT-U(pyr) amidite, 120 µl of 0.13 M of the amidite and 120 µl of 0.1 M tetrazole in acetonitrile (5 min) was used for the manual coupling. With these conditions, the coupling efficiency based on the DMT cation assay was 99% for each step in the normal phosphoramidite, whereas the coupling of the modified amidite was ~90%. The CPG bound oligonucleotides were treated with concentrated ammonium hydroxide at 55°C for 6 h. Purification of the modified oligomers was performed with reversed phase HPLC. DMT-oligonucleotides were purified by the elution conditions of CH_3CN (0.6%/min) gradient from 5% CH_3CN in 0.1 M triethylammonium acetate (pH 7.0) at a flow rate of 1.0 ml/min. The purified DMT-oligomers were treated with 80% acetic acid at room temperature for 30 min. Final purification by reversed phase HPLC was done with the same conditions above.

The modified oligonucleotides (0.1 A_{260} U) were subjected to digestion with nuclease P1 (8 U) and alkaline phosphatase (0.1 U) in 90 µl of 20 mM sodium acetate buffer (pH 4.9) containing 0.5 mM zinc sulfate at 37°C for 2 h. The reaction mixtures were directly analyzed by reversed phase HPLC. All pyrene-modified oligonucleotides gave nucleosides in expected ratio.

Preparation of oligonucleotide solutions for physical measurements

All solutions were prepared using a buffer containing 10 mM sodium phosphate and 100 mM NaCl, adjusted to pH 7.0. Oligonucleotide concentrations were determined on the basis of the measured absorbance at 260 nm after enzymatic digestion and ε values of nucleosides. UV-melting curves of the duplexes were obtained for solutions containing 1:1 strand ratio of oligonucleotides with an increase in temperature from 0 to 80°C at a rate of 0.5°C/min. CD spectra were measured for the same solutions used for the UV-melting studies. Fluorescence spectra were obtained at an excitation wavelength of 342 nm. Excitation spectra were measured by using the monitoring wavelength at 375, 380 and 450 nm. No attempt was made to eliminate dissolved oxygen in the buffer solution for the fluorescence measurements.

RESULTS

The synthesis of 2′-O-(1-pyrenylmethyl)uridine [U(pyr)] was accomplished by the published procedure (20). U(pyr) was converted by the usual method to a protected phosphoramidite which could be used for introduction of U(pyr) into the sequence of oligomer(pyr) **1**–**4**. The pyrene oligonucleotides were synthesized by a solid-phase phosphoramidite method, in which the coupling efficiency of 5′-DMT-U(pyr) amidite was ~90%. Purification of the pyrene oligonucleotides was done with a usual reversed phase HPLC and the base composition of purified oligomers was verified with enzymatic digestion analysis. The sequences of pyrene-modified oligonucleotides, DNA and RNA used in the present study are shown in Scheme 1. U(pyr) was placed in the center position of oligodeoxyribonucleotide 9mers which contain different bases at the 3′-site of U(pyr).

The binding of oligomer(pyr) **1**–**4** to their complementary DNA and RNA was investigated by UV-melting behaviours in aqueous neutral buffer solution. Figure 1a and b shows UV-melting curves at 260 nm for duplexes of oligomer(pyr) **1** with DNA **1** and RNA **1**, respectively. Both melting profiles exhibited sigmoidal curves whose shapes are similar to those for the

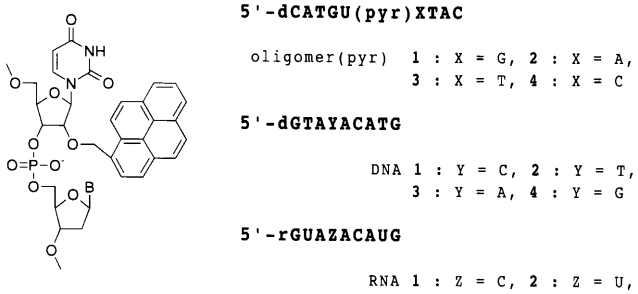

Scheme 1.

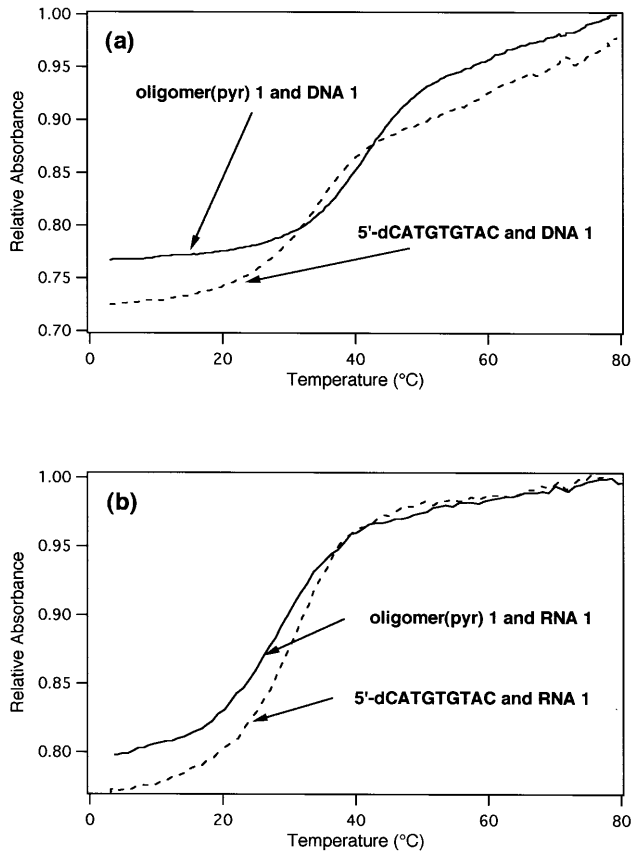

Figure 1. UV melting curves for duplexes of pyrene-modified oligonucleotide with (**a**) DNA and (**b**) RNA. Measurements were carried out at 260 nm for 1:1 mixture of oligonucleotides (6 μM each) in a buffer containing 10 mM sodium phosphate and 100 mM NaCl, adjusted to pH 7.0.

corresponding unmodified duplexes. The duplexes of oligomer(pyr) **2**–**4** showed similar melting profiles. The T_m values estimated from the UV-melting curves are summarized in Table 1. When compared with the unmodified oligonucleotides, the pyrene-modified oligonucleotides showed higher affinity for DNA while exhibiting lower affinity for RNA. The duplex stability was dependent on the sequence of the pyrene oligomers. The pyrene oligonucleotides **1** and **2** containing purine bases at the 3′-site of the modification afforded significantly stabilized DNA duplexes (ΔT_m 7 and 13°C). The oligomer(pyr) **3** and **4** containing pyrimidine bases at the same site showed relatively lower affinity for RNA (ΔT_m –10°C, respectively).

Table 1. T_m values for duplexes of pyrene-modified oligonucleotides with DNA and RNA

Duplex	T_m (°C)	ΔT_m (°C)[a]
oligomer(pyr) **1**–DNA **1**	41	+7
5′-dCATGTGTAC–DNA **1**	34	
oligomer(pyr) **2**–DNA **2**	37	+13
5′-dCATGTATAC–DNA **2**	24	
oligomer(pyr) **3**–DNA **3**	30	+2
5′-dCATGTTTAC–DNA **3**	28	
oligomer(pyr) **4**–DNA **4**	35	+2
5′-dCATGTCTAC–DNA **4**	33	
oligomer(pyr) **1**–RNA **1**	24	–5
5′-dCATGTGTAC–RNA **1**	29	
oligomer(pyr) **2**–RNA **2**	33	–1
5′-dCATGTATAC–RNA **2**	34	
oligomer(pyr) **3**–RNA **3**	14	–10
5′-dCATGTTTAC–RNA **3**	24	
oligomer(pyr) **4**–RNA **4**	20	–10
5′-dCATGTCTAC–RNA **4**	30	

[a]Values represent the differences of T_m values between pyrene-modified duplexes and the corresponding unmodified duplexes.
All measurements were carried out at 260 nm for 1:1 mixture of oligonucleotides (6 μM each) in a buffer containing 10 mM sodium phosphate and 100 mM NaCl, adjusted to pH 7.0.

Figure 2a and b shows the CD spectra for duplexes of oligomer(pyr) **1** with DNA **1** and RNA **1**, respectively. The CD profiles of the oligomer(pyr)–DNA duplex exhibited almost the same pattern as that for the unmodified duplex. The slight red-shift in both Cotton peaks at 250 and 270 nm was observed when compared with that of the B-form duplex. The oligomer(pyr)–RNA duplex showed a slightly altered CD pattern which resembles that for the unmodified DNA–RNA heteroduplex. In Figure 2c, expanded CD spectra for these pyrene-modified duplexes in the region between 300 and 380 nm are shown. The unmodified duplexes did not show any detectable peak in this region. The pyrene-modified oligonucleotide, however, exhibited peaks (335 and 350 nm) which are due to the pyrene chromophore, suggesting that the pyrene attached to the oligonucleotide was affected by the chiral environment. On binding of the pyrene oligonucleotide to DNA, the induced CD (ICD) peaks shifted to the longer wavelength with little change in their intensity. On the contrary, the duplex of the pyrene oligonucleotide with RNA showed relatively weak ICD with little peak shift. Similar changes in ICD upon hybridization were observed for all pyrene oligonucleotides studied here.

Fluorescence emission spectra for oligomer(pyr) **1** and its duplex with DNA **1** are shown in Figure 3a. The pyrene-modified oligonucleotide in diluted solution exhibited fluorescence typical of pyrene monomer emission [λ_{max} 378 (band I) and 391 nm (band III)]. Upon binding of this oligomer to DNA, the fluorescence intensity ratio of band III/band I, which is known to be strongly affected by local environmental polarity (24,25), was increased. With this fluorescence change, a new broad emission (λ_{max} 450 nm) appeared. The emission intensity at 450 nm was decreased with melting of the duplex, as shown in the inset in Figure 3a, and only the monomer emission was observed at the high temperature. The fluorescence changes were not observed for the pyrene oligonucleotides in the presence of non-complementary DNA sequence (data not shown). In Figure 3b, the

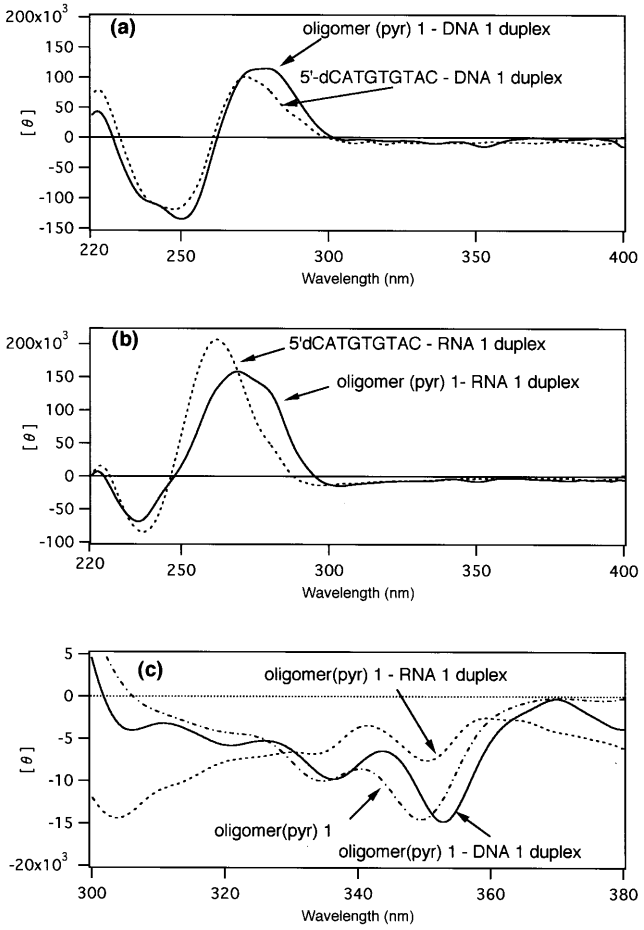

Figure 2. CD spectra for duplexes of pyrene-modified oligonucleotide with (**a**) DNA and (**b**) RNA. Expanded CD spectra for pyrene-modified oligonucleotide (6 μM) and its duplexes (6 μM each strand) are shown in (**c**). Measurements were carried out at 8°C in the same buffer described in Figure 1.

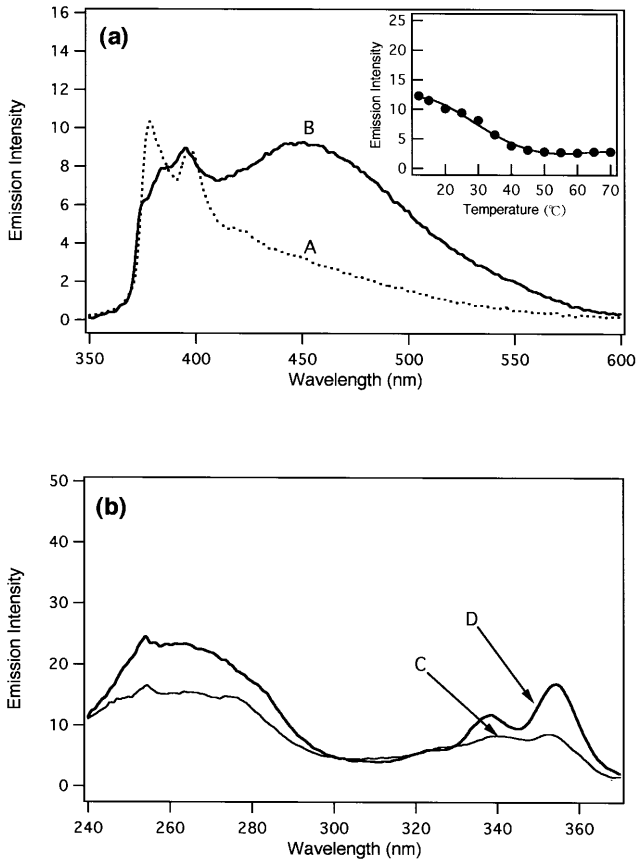

Figure 3. (**a**) Fluorescence emission spectra for oligomer(pyr) **1** (curve A) and its duplex with DNA **1** (curve B). The temperature dependent fluorescence changes at 450 nm for the duplex are shown in the inset. (**b**) Fluorescence excitation spectra for the oligomer(pyr) **1**–DNA **1** duplex obtained by using different monitoring wavelength [380 nm (curve C) and 450 nm (curve D)]. All measurements at single-strand concentration of 6 μM were carried out at 12°C in the same buffer described in Figure 1. Fluorescence spectra were recorded with an excitation wavelength of 342 nm.

excitation spectra of oligomer(pyr) **1**–DNA **1** duplex monitored for 450 and 380 nm are shown. The spectral patterns were different from each other, indicating that the emitting species for the exciplex emission were different from those for the monomer emission. Similar fluorescence properties were observed for oligomer(pyr) **2**–**4**, which are summarized in Table 2.

In contrast to the oligomer(pyr)–DNA duplexes, upon binding to RNA the pyrene oligonucleotides exhibited enhanced monomer emission with no new emission band. Figure 4a shows the fluorescence enhancement upon binding of oligomer(pyr) **1** with RNA **1**. With the large emission enhancement, the intensity ratio of band III/band I was decreased. The monomer emission intensity was decreased with the melting of the duplex as shown in the inset in Figure 4a and the weaker monomer emission was regenerated at the high temperature. The fluorescence changes were not observed for the pyrene oligonucleotides in the presence of non-complementary RNA sequence (data not shown). The fluorescence properties for all the pyrene oligonucleotides upon hybridization with RNA are summarized in Table 2. The extent of the emission enhancement was found to be highly dependent on the nucleobase adjacent to the U(pyr) in the pyrene oligomers. From a 1.3-fold increase in the fluorescence with the pyrene oligonucleotide **2** up to an enormous increase (250-fold) with oligomer(pyr) **4** containing dC at the 3′-site of the modification was observed. The excitation spectra for oligomer(pyr) **1** and its duplex with RNA are shown in Figure 4b. The excitation spectrum for the oligomer(pyr)–RNA duplex was clearly different from those for the pyrene oligomer itself as well as for the oligomer(pyr)–DNA duplex and appeared to resemble for the free pyrene in aqueous solution (26).

DISCUSSION

For all the pyrene-modified duplexes with DNA and RNA, the UV melting profiles exhibited sigmoidal curves or monophasic transitions whose shapes were similar to those for unmodified duplexes. Binding of the pyrene-modified oligonucleotides to DNA resulted in stabilized duplexes whose global conformation was similar to that of normal B-form double helix. On the contrary, the pyrene-modified oligonucleotides afforded relatively unstable RNA duplexes whose conformation resembled that of DNA–RNA heteroduplex. The relatively strong ICD observed at the region between 300 and 360 nm for the pyrene-modified DNA duplexes appeared to be consistent with the duplex stability. It is suggested that the mode of pyrene interaction in the modified DNA duplexes may be different from that in the modified RNA duplexes.

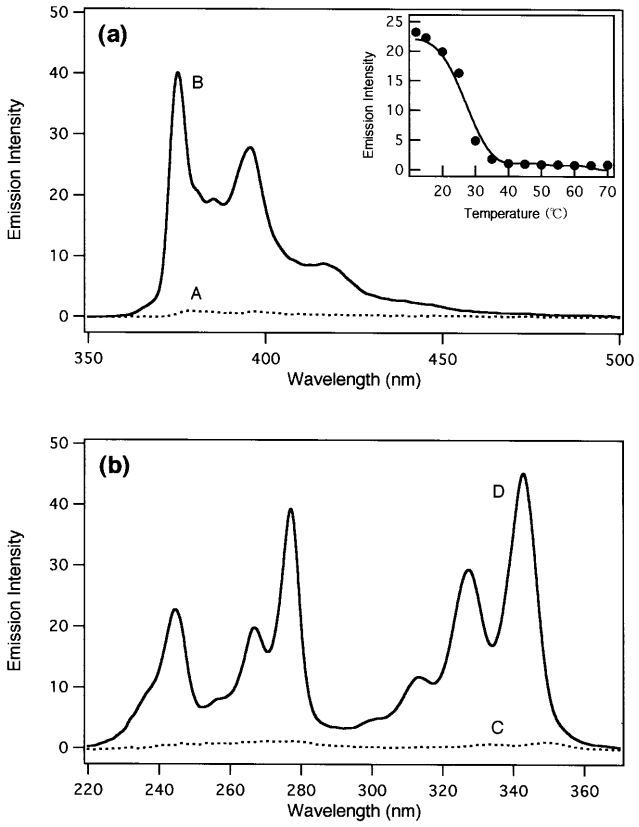

Figure 4. (**a**) Fluorescence emission spectra for oligomer(pyr) **1** (curve A) and its duplex with RNA **1** (curve B). The temperature dependent fluorescence changes at 380 nm for the duplex are shown in the inset. (**b**) Fluorescence excitation spectra for the oligomer(pyr) **1** (curve C) and its RNA duplex (curve D) obtained by using monitoring wavelength at 375 nm. Other conditions were described in Figure 3.

The pyrene-modified oligonucleotides in diluted solution exhibited fluorescence typical of pyrene monomer emission [λ_{max} 378 (band I) and 391 nm (band III)]. When these oligomers were bound to DNA, the fluorescence intensity ratio of band III/band I was increased. Since this intensity ratio is known to be increased with decrease in local environmental polarity (24,25), the pyrene is suggested to be transferred into more hydrophobic base-pair pocket upon hybrid formation of the pyrene oligonucleotides with DNA. The hybrid formation led to a new emission band observed at 450 nm. We ascribe this emission to the exciplex of the pyrene and adjacent base in the duplex. The possibility of phosphorescence emission by pyrene or nucleoside base can be ruled out, since the phosphorescence peak of pyrene is located at 600 nm and the phosphorescence spectrum of nucleoside bases (400–500 nm) is structured and extremely weak. The excitation spectrum of the exciplex emission was different from that of the monomer emission, indicating that most of the exciplex emission was derived from the pyrene strongly interacting with the nucleoside base. Since it is known that the uracil base is the best electron acceptor and the ionization potential of the polyaromatic hydrocarbons is generally lower than that of the bases (26–31), the most likely components of the exciplex are the uracil base as an electron acceptor and the pyrene as an electron donor.

In contrast to the oligomer(pyr)–DNA duplexes, the pyrene-modified oligonucleotide–RNA duplexes exhibited only monomer emission. Importantly, binding of the pyrene-modified oligonucleotides to RNA resulted in enhancement of the monomer emission as well as a decrease in the intensity ratio of band III/band I. As already discussed, the decrease in the intensity ratio indicates that the pyrene in the RNA duplex was located in the hydrophilic area or presumably outside of the duplex. The extent of the emission enhancement appeared to be consistent with the band ratio and was dependent on the nucleobase adjacent to the U(pyr) in the pyrene oligomers. The pyrene oligonucleotide–RNA duplexes containing a dC-dG pair at the 3′-site of the modification showed remarkable fluorescence enhancement upon binding to complementary RNA.

Table 2. Relative fluorescence emission intensity for pyrene-modified oligonucleotides and their duplexes with DNA and RNA

Pyrene oligonucleotide and duplex	Relative emission intensity at different λ_{max}			Ratio of intensity (band III/band I)
	378 nm (band I)	391 nm (band III)	450 nm	
oligomer(pyr) **1**	1.0	0.7	0.2	0.7
oligomer(pyr) **2**	1.3	1.8	1.5	1.4
oligomer(pyr) **3**	1.6	0.9	0.1	0.6
oligomer(pyr) **4**	1.7	1.1	0.4	0.7
oligomer(pyr) **1**–DNA **1**	0.5	0.8	0.8	1.6
oligomer(pyr) **2**–DNA **2**	1.5	3.0	2.1	2.0
oligomer(pyr) **3**–DNA **3**	0.8	1.7	1.5	2.1
oligomer(pyr) **4**–DNA **4**	0.4	0.7	0.9	1.8
oligomer(pyr) **1**–RNA **1**	46.0[a]	21.0[b]	–	0.5
oligomer(pyr) **2**–RNA **2**	1.7[a]	2.4[b]	–	1.4
oligomer(pyr) **3**–RNA **3**	21.0[a]	10.0[b]	–	0.5
oligomer(pyr) **4**–RNA **4**	421.0[a]	195.0[b]	–	0.5

[a]Measured at λ_{max} 375 nm (band I).
[b]Measured at λ_{max} 386 nm (band III).
All measurements were carried out for air-saturated solutions of pyrene-modified oligonculeotides (6 μM) in the presence or absence of complementary DNA and RNA (6 μM) in the same buffer used for UV melting measurements. Excitation wavelength was 342 nm.

CONCLUSION

Oligonucleotides containing a 2′-pyrene modified ribonucleoside exhibit interesting fluorescence properties upon binding to DNA and RNA. Intercalation of the pyrene in the DNA duplexes is compatible with the observations of stabilized duplex, strong ICD, large intensity ratio of band III/band I of the monomer emission, and exciplex emission. The location of the pyrene outside the duplex with RNA is consistent with the observations of unstable duplex, weak ICD, small band intensity ratio and enhanced monomer emission. In addition, the enhanced emission in the RNA duplex is derived from the pyrene free from interactions (with nucleoside bases), which is strongly suggested by the excitation spectral analysis.

The largely enhanced fluorescence upon binding of an oligonucleotide probe to RNA has found several applications such as investigation of ribozyme reaction (19) and monitoring of *in vitro* transcription (6) in homogeneous systems. Our pyrene oligonucleotides exhibit enhanced fluorescence upon binding to RNA. The fluorescence enhancements are highly dependent on the local sequences around the pyrene modification in RNA duplexes. The extent of the enhancement was up to 250-fold with an appropriate choice of the sequence. This property may lead to a high sensitivity in solution-based analysis of RNA. The relatively low affinity of the pyrene oligonucleotides for RNA might cause little problems with long-chained pyrene oligonucleotides in RNA sequence and structural analysis. Further research to evaluate the potential and limitation of the pyrene oligonucleotides by use of long and different sequences is in progress.

ACKNOWLEDGEMENTS

This research was partially supported by Termo Life Science Foundation (A.M.) and Grant-in-Aid for Scientific Research on Priority Areas no. 09255230 and 09273236 (A.M., T.Y. and R.I.) from the Ministry of Education, Science, Sports and Culture of Japan.

REFERENCES

1 Murakami,A., Nakaura,M., Nakatsuji,Y., Nagahara,S., Tran-Cong,Q. and Makino,K. (1991) *Nucleic Acids Res.*, **19**, 4097–4102.
2 Cardullo,F., Agrawal,S., Flores,C., Zamecnik,P.C. and Wolf,D.E. (1988) *Proc. Natl Acad. Sci. USA*, **85**, 8790–8794.
3 Morrison,L.E., Halder,T.C. and Stols,T.S. (1989) *Anal. Biochem.*, **183**, 231–244.
4 Oser,A. and Valet,G. (1990) *Angew. Chem. Int. Ed. Engl.*, **29**, 1167–1169.
5 Mergny,J.L., Garestier,T., Rougee,M., Alexandre,A.V., Chassignol,M., Thoung,N.T. and Hélène,C. (1994) *Biochemistry*, **33**, 15321–15328.
6 Ishiguro,T., Saitoh,J., Yawata,H., Otsuka,M., Inoue,T. and Sugiura,Y. (1996) *Nucleic Acids Res.*, **24**, 4992–4997.
7 Jenkins,Y. and Barton,J.K. (1992) *J. Am. Chem. Soc.*, **114**, 8736–8738.
8 Wiederholt,K., Rajur,S.B., Giuliano,J.,Jr, O'Donnell,M.J. and McLaughlin,L.W. (1996) *J. Am. Chem. Soc.*, **118**, 7055–7062.
9 Yamana,K., Ohashi,Y., Nunota,K. and Nakano,H. (1997) *Tetrahedron*, **53**, 4265–4270.
10 Paris,P.L., Langenhan,J.M. and Kool,E.T. (1998) *Nucleic Acids Res.*, **26**, 3789–3793.
11 Lewis,F.D., Zhang,Y. and Letsinger,R.L. (1997) *J. Am. Chem. Soc.*, **119**, 5451–5452.
12 Yamana,K., Takei,M. and Nakano,H. (1997) *Tetrahedron Lett.*, **38**, 6051–6054.
13 Ebata,K., Masuko,M., Ohtani,H. and Jibu,M. (1995) *Photochem. Photobiol.*, **62**, 836–839.
14 Tong,G., Lawlor,J.M., Tregear,G.W. and Haralambidis,J. (1995) *J. Am. Chem. Soc.*, **117**, 12151–12158.
15 Mann,J.S., Shibata,Y. and Meehan,T. (1992) *Bioconj. Chem.*, **3**, 554–558.
16 Telser,J., Cruickshank,K.A., Morrison,L.E. and Netzel,T.L. (1989) *J. Am. Chem. Soc.*, **111**, 6966–6976.
17 Yamana,K. and Letsinger,R.L. (1985) *Nucleic Acids Symp. Ser.*, **16**, 169–172.
18 Kierzek,R., Li,Y., Turner,D.H. and Bevilacqua,P.C. (1993) *J. Am. Chem. Soc.*, **115**, 4985–4992.
19 Bevilacqua,P.C., Kierzek,R., Johnson,K.A. and Turner,D.H. (1992) *Science*, **258**, 1355–1358.
20 Yamana,K., Ohashi,Y., Nunota,K., Kitamura,M., Nakano,H., Sangen,O. and Shimidzu,T. (1991) *Tetrahedron Lett.*, **32**, 6347–6350.
21 Yamana,K., Gokota,T., Ozaki,H., Nakano,H., Sangen,O. and Shimidzu,T. (1992) *Nucl. Nucl.*, **11**, 383–390.
22 Iwase,R., Furutani,S., Yamaoka,T., Yamana,K. and Murakami,A. (1996) *Nucleic Acids Symp. Ser.*, **35**, 117–118.
23 Iwase,R., Tsuchida,H., Yamaoka,T., Yamana,K. and Murakami,A. (1997) *Nucleic Acids Symp. Ser.*, **37**, 205–206.
24 Kalyanasundaram,K. and Thomas,J.K. (1977) *J. Am. Chem. Soc.*, **99**, 2039–2044.
25 Nakajima,A. (1971) *Bull. Chem. Soc. Jpn*, **44**, 3272–3277.
26 Cho,N. and Asher,S.A. (1993) *J. Am. Chem. Soc.*, **115**, 6349–6356.
27 Oyler,N.A. and Adamowicz,L. (1994) *Chem. Phys. Lett.*, **219**, 223–227.
28 Steenken,S., Telo,J.P., Novais,H.M. and Candeias,L.P. (1992) *J. Am. Chem. Soc.*, **114**, 4701–4709.
29 Colson,A.-O., Besler,B., Close,D.M. and Sevilla,M.D. (1992) *J. Phys. Chem.*, **96**, 661–668.
30 Jovanovic,S.V. and Simic,M.G. (1986) *J. Phys. Chem.*, **90**, 974–978.
31 Geacintov,N.E., Prusik,T. and Khosrofian,J.M. (1976) *J. Am. Chem. Soc.*, **98**, 6444–6452.